Effects of Orthotropy and Width on the Compression Strength of Graphite-Epoxy Panels with Holes

Marvin D. Rhodes,* Martin M. Mikulas Jr.,† and Paul E. McGowan‡
NASA Langley Research Center, Hampton, Virginia

An experimental study was conducted to evaluate the effect of laminate orthotropic properties and panel width on the compression strength of 48-ply graphite-epoxy laminates with drilled holes. The test results were evaluated on the basis of hole size and specimen width and were used to determine parameters necessary to predict trends using the point-stress failure criterion. Good agreement was obtained between experimental and predicted values of failure for panels fabricated from two quasi-isotropic laminates and one orthotropic laminate. The results indicate that panels of different widths that have large holes in relation to the failure prediction parameter should be included in any test program conducted to develop predictions. Panel failures are shown to have an upper limit given by the reduction in specimen cross-sectional area and a lower limit given by the effect of stress concentration. Limited tests of a quasi-isotropic laminate were conducted on panels with machined cracks and panels with punched holes and the results compared to those with drilled holes. The sequence of events that occurs in the vicinity of a hole during failure was identified and provides insight into the mechanisms associated with failure.

Nomenclature

a	= notch size, specifically hole diameter or crack length, cm
d	= parameter associated with the point-stress failure criterion, radial distance from the edge of a notch to the point where the stress reaches the critical value, cm
E_x, E_y	= longitudinal and transverse elastic moduli of test specimens, Pa
G_{xy}	= elastic shear modulus of graphite-epoxy test specimens, Pa
K_T	= gross area stress concentration factor
W	= panel width, cm
x, y	= coordinate axes
ϵ_F	= applied far-field strain at failure
ν_{xy}	= major Poisson's ratio of test laminates
σ_A	= far-field stress in the direction of the applied load, Pa
σ_{AF}	= far-field stress in the direction of the applied load at failure, Pa
σ_{ULT}	= ultimate strength of a defect free material, Pa
σ_y	= local stress in the direction of the applied load, Pa

Introduction

EXPERIMENTAL studies of compression-loaded filamentary composite structures indicate that severe strength reductions can occur due to defects caused by impact damage.[1-3] Such studies have demonstrated the need to develop a failure prediction technique which can reliably account for the observed failure trends. The first step in developing a general prediction technique for damage is an examination of prediction techniques for well-defined shapes such as holes that can be analyzed mathematically.

Failure prediction techniques for laminated plates with holes loaded in tension have been explored by a number of investigators and several studies are reported in Refs. 4-7. Two of these prediction techniques have been extended to include compression loaded laminates,[8,9] however, these studies focused only on small holes typical of those used for aircraft fasteners. In Ref. 10, the point-stress failure criterion for compression applications was examined for general hole sizes and specimen widths. Although good results were obtained in the Ref. 10 study, only one laminate was examined.

The present experimental investigation was conducted to expand the limited data base of Ref. 10 and to evaluate other laminate configurations. Quasi-isotropic and orthotropic laminates with several different specimen widths and hole sizes were tested. Most tests were conducted on 48-ply filament-controlled graphite-epoxy tape laminates. The test results presented herein for both the quasi-isotropic and orthotropic laminates are evaluated parametrically on the basis of hole size and specimen width and compared with predicted trends using the point-stress failure criterion. Experimental studies were also conducted on laminates with

Table 1 Typical properties of unidirectional graphite-epoxy systems

Material property	Material A	Material B
Longitudinal compression strength, GPa	1.45	1.24
Longitudinal compression modulus, GPa	131.0	112.4
Transverse modulus, GPa	13.0	–
Shear modulus, GPa	6.4	–
Poisson's ratio (major)	0.38	–
Short beam shear strength, MPa	131.0	106.9
Fiber volume fraction	0.71	0.68
Neat resin elongation to failure	0.010	0.048
Average ply thickness, mm	0.14	0.15

Presented as Paper 82-0749 at the AIAA/ASME/ASCE/AHS 23rd Structures, Structural Dynamics and Materials Conference, New Orleans, La., May 10-12, 1982; received June 7, 1982; revision received Jan. 3, 1984. This paper is declared a work of the U.S. Government and therefore is in the public domain.

*Aerospace Engineer, Structural Concepts Branch, Structures and Dynamics Division. Member AIAA.

†Head, Structural Concepts Branch, Structures and Dynamics Division. Member AIAA.

‡Presently, Engineering Cooperative Student, Old Dominion University, Norfolk, Virginia.

Table 2 Ply orientation of test specimens and calculated elastic properties based on material A lamina properties

Laminate designation	Quasi-isotropic			Orthotropic
Ply orientation	$(\pm 45/0/90/\mp 45/0/90)_{3s}$	$(\pm 60/0/\mp 60/0)_{4s}$	$(\pm 30/90/\mp 30/90)_{4s}$	$(\pm 45/0_2/\pm 45/0_2/\pm 45/0/90)_{2s}$
No. of plies	48	48	48	48
Thickness, cm	0.67	0.67	0.67	0.67
Longitudinal modulus, GPa	53.3	53.3	53.3	70.2
Transverse modulus, GPa	53.3	53.3	53.3	34.8
Shear modulus GPa	20.2	20.2	20.2	20.2
Major Poisson's ratio	0.32	0.32	0.32	0.48

through cracks, and the results are compared to those with holes to evaluate the effect of damage shape. Several test specimens loaded to near failure were examined by destructive inspection techniques to determine the sequence of events that occurs in the vicinity of a hole prior to failure. This paper discusses the use of the point-stress failure technique with regard to structural design and its application to the development of ancillary test results. The results presented herein are also examined for use in predicting strength failures associated with damage introduced by impact.

Test Specimens and Procedure

Materials

The specimens used in this investigation were fabricated from graphite-epoxy tape materials. The graphite fiber incorporated in the tape is Thornel 300§ a commercially available, high-strength, continuous, unidirectional, filamentary material. The tape was purchased from vendors with the epoxy preimpregnated and was kept refrigerated in sealed containers until ready for use. Two commercially available 450 K cure thermosetting epoxy-resin systems were evaluated. Representative properties for unidirectional composites fabricated using these two resin systems were obtained from Refs. 1 and 11 and are given in Table 1. The resin system in material A (Rigidite 5208¶) is a widely used system with high-flow characteristics during the cure process. It was chosen because it is representative of systems used in many secondary aircraft flight structures. Material B (Cycom 907**) has low-flow characteristics during the cure process and was chosen because it has good impact damage tolerance.[12]

Specimens

All specimens were flat rectangular plates cut from 48-ply laminates. Four different ply orientations were examined, and the calculated elastic properties based on material A lamina properties and the ply orientations are given in Table 2. Three of the ply orientations have quasi-isotropic elastic properties and the fourth is orthotropic with a longitudinal to transverse modulus ratio of 2.0. All specimens were fabricated in large plates using conventional fabrication procedures and the plates were autoclave cured. Following cure, the plates were inspected ultrasonically to ensure freedom from disbonds and foreign inclusions. The test specimens were cut from the plates using diamond-impregnated tooling, and the ends to be loaded were ground flat and parallel.

A range of hole sizes was tested for several specimen widths for both the quasi-isotropic and orthotropic panels. The test parameters and specimen dimensions are given in Table 3. Three types of specimens (see heading labeled Notch Type) were evaluated: specimens with drilled holes, specimens with punched holes, and specimens with cracks. The drilled holes, punched holes, and cracks subsequently are referred to collectively as notches. All notches were located in the center of the specimen. The drilled holes were machined using diamond-impregnated core bits to minimize fiber damage at the hole boundary. The punched holes were formed using a conventional hydraulic punch press, and each punched specimen was inspected ultrasonically following the punching operation to determine the damage in the region surrounding the hole. The cracks were machined using ultrasonic techniques.

Some of the specimens had strain gages bonded to the surface to evaluate the axial strain distribution along a horizontal line between the edge of the hole and the side of the specimen. These gages were approximately 0.3 mm wide by 1.8 mm long.

Procedure

The test specimens were supported in frames which consisted of two adjustable side supports and adjustable end supports at the top and bottom. The side supports simulate simple-support boundary conditions and were placed approximately 0.6 cm from the specimen edge. The adjustable end supports simulate clamped boundary conditions. The frame used to test panels 38.1-cm wide had two interior supports located at the one-third points to suppress a panel buckling mode of one-half wavelength across the specimen width. These interior supports were placed on each side of the specimen. Both test frames were placed in conventional hydraulic loading machines and the specimens were loaded to failure in compression.

One unnotched specimen, 12.7-cm wide by 25.4-cm long, from each fabricated plate was instrumented with strain gages and tested to measure the stress-strain behavior. The elastic modulus was obtained from the test data and compared to both the calculated value and the values measured during tests on other plates of the same ply orientation. An average value of longitudinal modulus, the specimen dimensions, and the failure load were used to calculate the far-field strain at failure. This procedure served as a quality control techique for the fabricated plates and established a common basis for reducing and evaluating test results.

Most of the specimens with notches were loaded in compression to failure. However, several specimens with holes were tested by loading the specimen to near the predicted failure load and then removing the specimen from the test frame. These specimens were sectioned in the vicinity of the hole using a diamond-impregnated saw, and the cross sections were examined with optical and scanning electron microscopes. Abrasive papers were used on several panels to

§Thornel 300 is a trade name of Union Carbide Corporation. Identification of commercial products and companies in this report is used to describe adequately the test materials. The identification of these commercial products does not constitute endorsement, expressed or implied, of such products by the National Aeronautics and Space Administration or the publisher.

¶Rigidite 5208 is a trade name of Narmco Materials Corporation.

**Cycom 907 is a trade name of American Cyanamid Corporation.

Table 3 Test parameters and specimen dimensions

Specimen	Material	Ply orientation	Notch type	Specimen width, cm	Specimen length, cm	Range of hole sizes, a/w	No. of specimens tested
A1	A	$(\pm 45/0/90/\mp 45/0/90)_{3s}$	Drilled holes	2.5	25.4	0.06—0.75	16
A2	A	↓	↓	5.1	25.4	0.02—0.50	19
A3	A	↓	↓	12.7	25.4	0.05—0.50	9
A4	A	↓	↓	38.1	25.4	0.05—0.10	3
A5	A	$(+45/90/0\pm 45/90/0)_{3s}$	↓	25.4	38.1	0.30	1
A6	A	$(\pm 45/0_2/\pm 45/0_2/\pm 45/0/90)_{2s}$	↓	5.1	25.4	0.05—0.50	5
A7	A	↓	↓	11.4	25.4	0.05—0.50	9
A8	A	↓	↓	38.1	25.4	0.02—0.10	3
A9	A	↓	↓	38.1	50.8	0.20	1
A10	A	$(\pm 45/0/90/+45/0/90)_{3s}$	Machined cracks	12.7	25.4	0.02—0.64	13
A11	A	$(\pm 60/0/+60/0)_{4s}$	Drilled holes	12.7	25.4	0.02—0.40	6
A12	A	$(\pm 30/90/+30/90)_{4s}$	Drilled holes	12.7	25.4	0.02—0.40	6
A13	A	$(\pm 45/0/90/+45/0/90)_{3s}$	Punched holes	12.7	25.4	0.03 – 0.40	7
B1	B	↓	Drilled holes	12.7	25.4	0.02 – 0.45	7
B2	B	↓	Machined cracks	12.7	25.4	0.05 – 0.64	8
B3	B	↓	Punched holes	12.7	25.4	0.03 – 0.25	5

remove plies near the hole so that interior regions of the laminate could be inspected.

Analysis

The point-stress failure criterion used to correlate the test data has been discussed by a number of authors. A similar theory was presented by Waddoups et al.[4] to explain hole size effects on laminate failure. The rationale for that study was based on linear-elastic fracture mechanics. A subsequent study by Whitney and Nuismer[5] developed the hypothesis for the point-stress failure criterion on the basis of the influence that hole diameter has on the stress distribution just ahead of the hole in an infinite plate. A perspective on the effect of finite width on specimen failure was presented by Mikulas.[10] Selected results from Refs. 5 and 10 are included in the subsequent discussion for completeness.

Failure Criterion Development

Test results on filament-controlled graphite-epoxy laminates (laminates with some plies in the direction of the applied load) indicate that these materials exhibit brittle behavior because plots of the stress-strain data are nearly linear to failure. Plates with circular holes fabricated from filament-controlled laminates might be expected to fail when the stress adjacent to the hole reaches the ultimate strength of the material. For plates fabricated from ideally brittle materials with small holes, the applied stress at failure would be the material strength divided by the stress concentration factor, and the applied stress at failure would be insensitive to small changes in hole diameter. The experimental results from tests on graphite-epoxy composite plates with small holes presented in Ref. 13, however, indicate the applied stress at failure is generally well above the value one might predict by the stress concentration factor and the applied stress at failure is very sensitive to small changes in hole diameter.

Several explanations for the composite panel results noted above can be postulated. First, the fibers in the vicinity of the hole boundary may be damaged by the drilling operation which makes the effective hole diameter larger than the nominal measured value. Second, composites are heterogeneous materials, and therefore, may not develop the local stress distribution in the vicinity of a hole which is mathematically postulated for homogeneous materials. Third, the stresses on the hole boundary are high and are influenced by interlaminar free-edge effects.[14] The high stress at the boundary may initiate local failures which result in a redistribution of stresses.

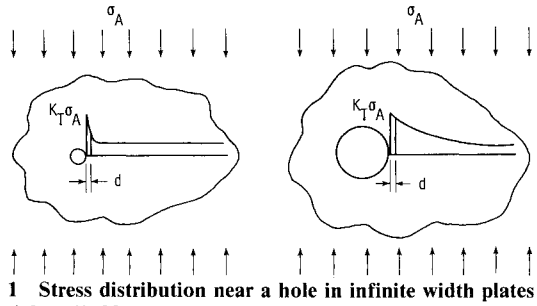

Fig. 1 Stress distribution near a hole in infinite width plates due to uniaxial applied load.

The local effects around a hole noted previously are difficult to define mathematically, however, they may be accounted for heuristically by the point-stress failure criterion without knowing the exact material response. The point-stress failure criterion is based on the premise that failure occurs when the stress at a small distance d away from the hole edge reaches the ultimate strength of the material. The sensitivity of the applied stress at failure to small changes in hole diameter can be explained on the basis of the point-stress failure criterion using the stress distributions in Fig. 1. Shown in Fig. 1 are the stress distributions for two hole diameters in infinite width plates for a quasi-isotropic homogeneous material as determined by the equation

$$\sigma_y = \sigma_A \left[1 + \frac{1}{2}\left(\frac{a}{2x}\right)^2 = \frac{3}{2}\left(\frac{a}{2x}\right)^4\right]$$

(see Ref. 15). Also shown in Fig. 1 is a fixed distance d adjacent to the hole as defined by the point-stress failure criterion. The maximum stress at the hole boundary ($K_T\sigma_A$) is the same for both hole sizes, however, the stress distribution indicates that a large region is at a high stress state in the panel with the larger hole. Therefore, it is less likely that local stress

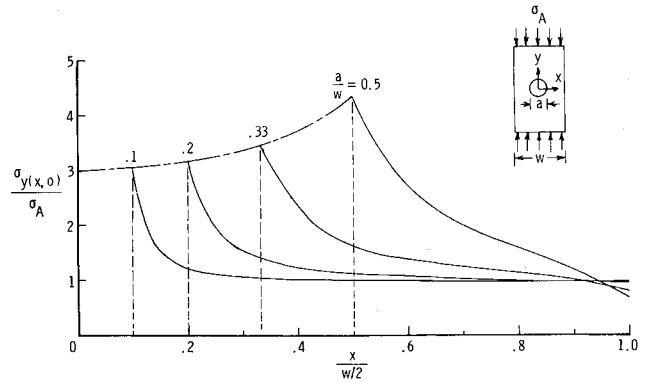

a) Quasi-isotropic laminate.

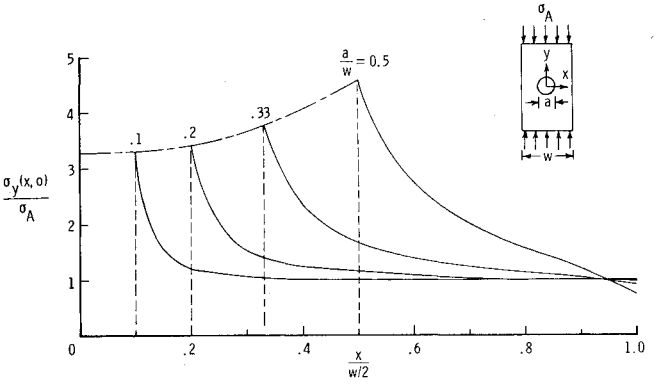

b) Orthotropic laminate.

Fig. 2 Distribution of axial stress in the vicinity of a hole for finite width plates of quasi-isotropic and orthotropic homogeneous materials.

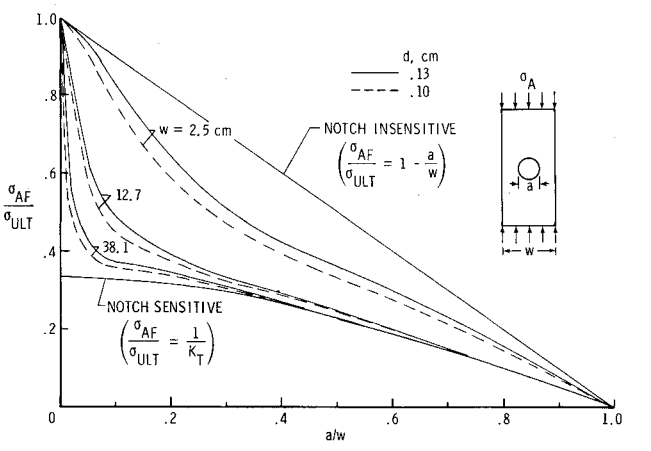

a) Effect of varying hole diameter.

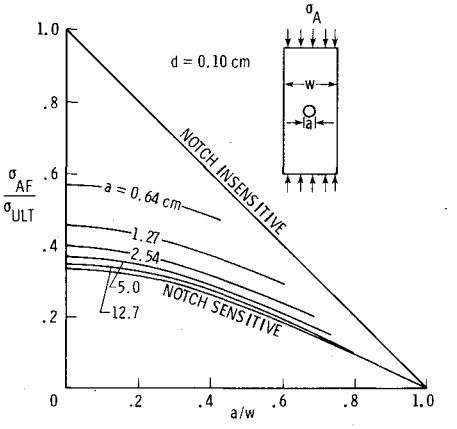

b) Effect of varying plate width.

Fig. 3 Predicted failure stress for quasi-isotropic plates as determined using the point-stress failure criteria.

relief or stress redistribution can occur in panels with large holes before the applied stress reaches a critical value. The preceding discussion disregards finite width effects and only considers wide panels or panels that can be considered of infinite width relative to hole diameter. When panel width effects are included in the analysis it is apparent that hole size influences both the stress distribution and the stress concentration. For example, the stress distributions for the two classes of laminates evaluated experimentally in this investigation are shown in Fig. 2 for a number of hole diameters. The distributions were obtained assuming homogeneous material properties using the finite element analysis code and model described in Ref. 16. These plots indicate that panels with small holes (a/w less than 0.1) have stress distributions and stress concentration factors similar to those of an infinite plate (Fig. 1), however, panels with large holes (a/w greater than 0.33) have stress distributions and stress concentrations that differ significantly from those of the infinite plate. Therefore, accurate stress distributions which account for finite width effects should be obtained before the point-stress failure prediction technique is applied to composite laminates with holes.

Failure Prediction

Experimental studies are conducted frequently to evaluate the effect of holes on laminates used in structural applications. Generally the investigator varies hole diameter using specimens of constant width, or keeps hole diameter constant and varies the width of the specimens. Experimental programs are costly, and it is desirable to use limited test results to predict the failure strength of panels over a general range of hole sizes and panel widths. The point-stress failure criterion was used as a convenient technique to examine hole size and width effects in the current investigation. The stress distributions of Fig. 2 and selected values of d were used to show the trends of predicted failure stress for quasi-isotropic plates and the results are presented in Fig. 3. The effect of varying hole diameter using plates of constant width (for three plate widths) is shown in Fig. 3a and the effect of holding the hole diameter constant and varying the plate width (for five hole diameters) is shown in Fig. 3b. The figure ordinates are the applied stress at failure normalized by the ultimate material strength, and the abscissas are the ratios of the hole diameter to specimen width. Each curve on Fig. 3 was faired through points which are the reciprocals of the normalized stress obtained at points on the stress distributions shown in Fig. 3 using the specified value of d.

Included on the plots (Fig. 3) are curves labeled "notch sensitive" and "notch insensitive" which are limiting cases for strength failures of plates with holes. These limiting cases are illustrated in Fig. 4. The panel in Fig. 4 labeled notch insensitive represents a specimen fabricated from a material that exhibits local relief at the hole edge so that there is no apparent effect of the stress concentration. For materials that exhibit this behavior, the applied stress at failure is directly proportional to the reduction in the area of the cross section. The panel labeled notch sensitive represents a panel fabricated from a material that is ideally brittle and fails when the stress at the hole edge due to the stress concentration reaches the ultimate strength of the material. Other failure criteria (for example, see Refs. 9 and 17) have been postulated for composite plates and the location of the failure point determined by other criteria does not necessarily occur at the same point where the stress concentration is a maximum. For this investigation, the notch sensitive and notch insensitive cases are assumed to represent the extremes of material

behavior and all flat uniaxially loaded panels with holes that exhibit strength controlled failures should lie between the bounds of these curves.

The normalized failure stress represented by the curves in Fig. 3a is shown for two values of d (0.13 and 0.10 cm). The curves in Fig. 3 illustrate that specimen dimensional parameters (specimen width when varying hole diameter, and hole diameter when varying specimen width) have a significant effect on interpreting whether a material is notch sensitive or notch insensitive and on the failure strength that can be expected in structural applications.

Comparison of Holes and Cracks

In examining any failure prediction technique that might have application to damage of a general nature, it is of interest to evaluate the prediction capability for different notch shapes to determine the range of applicability of the technique. A preliminary comparison of the effect of holes and cracks with the hole diameters equal to the crack lengths was conducted to provide insight into the effect of notch shapes. The stress distributions for three hole diameters and crack widths in a quasi-isotropic plate of infinite width are shown in Fig. 5. The ordinate is the normal stress near the edge of the notch divided by the applied stress, and the abscissa is the distance from the edge of the notch. The stress distributions for the holes are similar to those shown in Fig. 1 and were obtained using the equation presented previously, while the distributions for the crack were obtained from the equation below (Ref. 18).

$$\sigma_y = \sigma_A \frac{x}{\sqrt{x^2 - (a/z)^2}}$$

where $x = \bar{x} + a/2$ (see Fig. 5).

Considerable insight into the relative behavior of holes and cracks in wide plates can be inferred by comparing these stress distributions. For all hole sizes the stress at the hole edge is limited to three times the applied far-field stress, while the crack has an unlimited stress due to the singularity at the crack edge. For the smallest hole and crack shown in the figure ($a = 0.25$ cm), the stress distributions are quite similar except near the crack tip; however, there are considerable differences in the hole and crack distributions for the 25-cm-wide notches even at large distances from the crack tip. Also shown on the figure is a distance d of 0.13 cm where the failure stress might be evaluated using the point-stress failure criterion. This is the same value of d used in the discussion of Fig. 3a and is close to the value obtained by fitting the point-stress criterion to the experimental data obtained in the present investigation. An examination of the stress distributions with regard to the location of d indicates that the predicted value for failure using the point-stress criterion would be about the same for cracks and holes with values of a less than 2.5 cm. For larger cracks, the local stress at the location corresponding to $d = 0.13$ is higher than that of a hole of the same diameter, consequently, a specimen with a crack will have a lower applied stress at failure than a similar specimen with a hole.

Predicted values of failure stress based on a value of $d = 0.13$ cm for infinite width plates are shown in Fig. 6 as a function of notch size. For values of notch size greater than about 2.5 cm, a specimen with a crack will have a lower strength than a specimen with a hole. This difference in strength between plates with cracks and plates with holes becomes more pronounced for larger notches in wide plates.

Results

The test results of the current investigation and data from studies reported in the literature are presented in this section. The strain distribution measured on several panels is compared with analytically predicted strain values. The strain at failure for several quasi-isotropic laminates with drilled holes

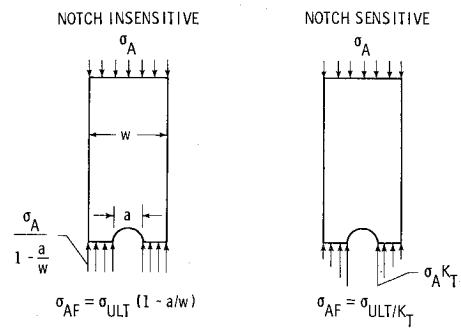

Fig. 4 Limiting cases for failure of plates with holes.

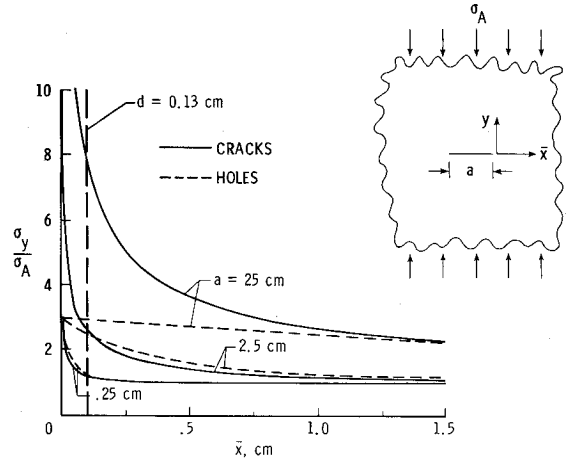

Fig. 5 Stress distributions at the edge of a hole and a crack for infinite width quasi-isotropic plates.

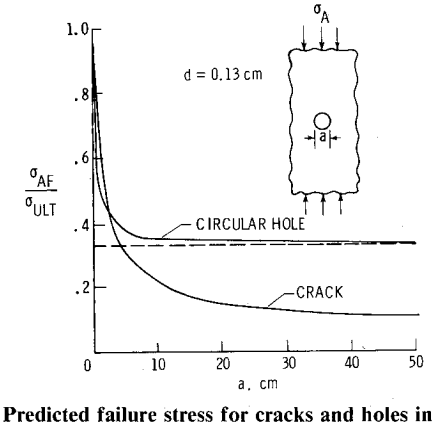

Fig. 6 Predicted failure stress for cracks and holes in infinite width plates as a function of notch size.

and an orthotropic laminate with drilled holes, all fabricated from material A, are presented for several different panel widths and hole sizes. The applied strain at failure for the quasi-isotropic and orthotropic laminates is correlated using the point-stress failure criterion. Results for quasi-isotropic panels with drilled holes, punched holes, and machined cracks fabricated from material B are presented, and the test results compared with corresponding data from panels fabricated from material A.

Measured Strain Distributions

The strain distribution in the vicinity of the hole was measured for four different hole diameters on 11.4-cm-wide orthotropic plate specimens, and the results are shown in Fig. 7. The measured values were obtained at an applied axial strain of 0.0026 which is well below the failure strain for any

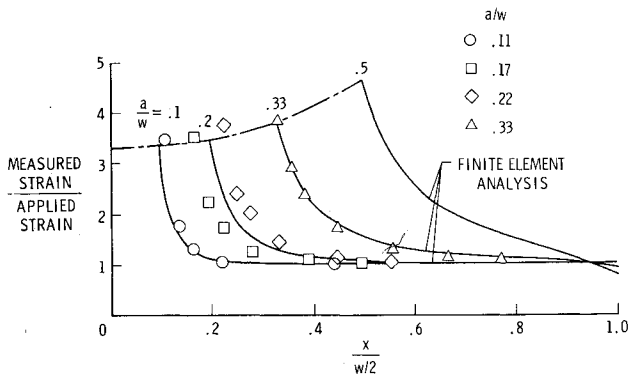

Fig. 7 Axial stresses measured in the vicinity of a hole for several hole diameters in 11.4-cm-wide orthotropic plate specimens.

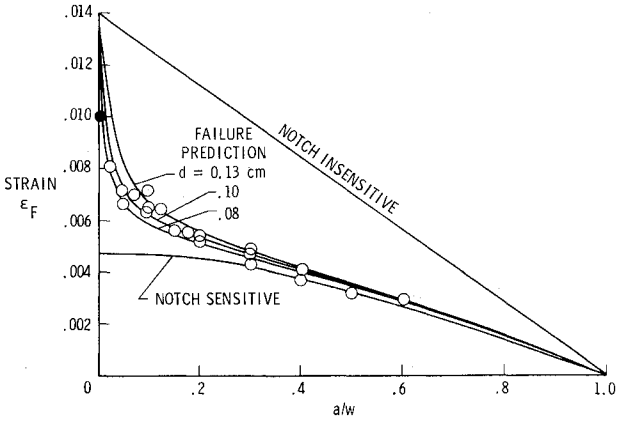

a) 12.7-cm-wide test panels, specimen A3 and data from Ref. 17.

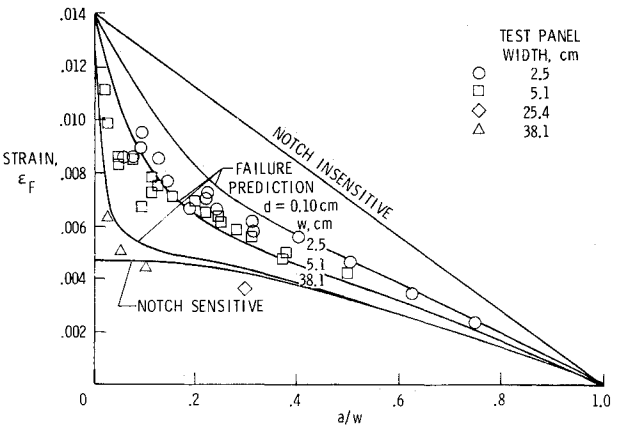

b) 2.5-cm-wide test panels, specimen A1; 5.1-cm-wide test panels, specimen A2; 38.1-cm-wide test panels, specimen A4; and 25.4-cm-wide test panel, specimen A5.

Fig. 8 Failure strain of a quasi-isotropic laminate fabricated from material A as a function of hole size.

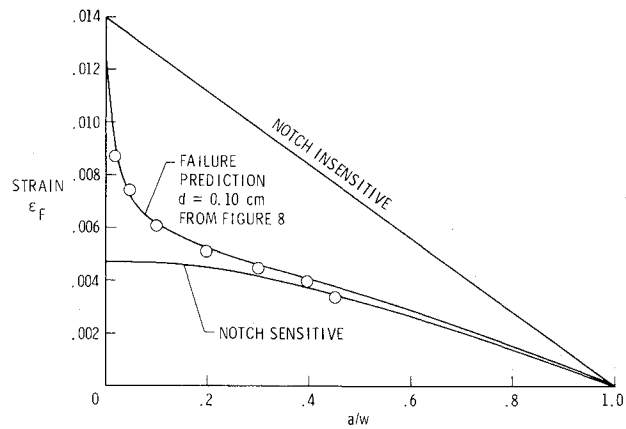

Fig. 9 Failure strain of a quasi-isotropic laminate fabricated from material B as a function of hole size.

of the specimens. The measured values and distributions compare favorably with those predicted by the finite element model which are also shown on Fig. 7. These results indicate that the stress distributions (Fig. 2) necessary for application of the point-stress failure criterion are accurate representations of the distributions that occur in the test panels.

Quasi-Isotropic Laminates with Holes

The applied strain at failure for quasi-isotropic test panels fabricated from material A is shown in Fig. 8 as a function of hole size for several panel widths (specimens A1-A5 in Table 3). All of the data shown in Fig. 8 were obtained in the current investigation with the exception of 11 of the 20 data points on Fig. 8a. These 11 points were obtained from Ref. 19, however, the experimental studies of Ref. 19 were performed in the same laboratory using the same facilities and procedure as the present investigation. Also shown on the figure are the notch sensitive and notch insensitive bounding curves as well as curves based on the point-stress failure criterion. Three values of the parameter d were selected to compare the failure prediction technique with the test data shown in Fig. 8a, and the value of 0.10 cm appears to provide the best fit for these 12.7-cm-wide panels. Panels of this width were used to determine the value of d because more data were available than for panels of other widths. The same value of d (0.10 cm) was then used to define failure prediction curves for the other panel widths (Fig. 8b). A curve based on a 25.4-cm-wide panel for specimen A5 is not shown since it would be only slightly above the curve shown for the 38.1-cm-wide panels. Although all of the test points for Figs. 8a and 8b do not lie on the predicted failure curves, the trends in the data agree with the trends of the failure prediction curves. Note that the test panel associated with the filled symbol on Fig. 8a did not contain a hole and failed after panel buckling. Consequently, it does not represent a simple material strength failure.

Discrepancies between the data points and the prediction curves may be due to a number of factors. First, the failure prediction technique is based on a heuristic evaluation to account for observed trends as opposed to a mathematically supported theory. Second, the prediction depends on the ultimate strain value. The ultimate strain of the test laminates was assumed to be 0.014 for these calculations. The selection of a different ultimate strain value will shift the location of the failure prediction curves. It is difficult to obtain an accurate value of the ultimate compression strain of a filament-controlled composite laminate because test results are influenced significantly by test techniques and specimen supports. Values of ultimate strain as high as 0.016 have been reported[20] for a quasi-isotropic graphite-epoxy laminate. Other values of ultimate strain were examined for failure prediction, but 0.014 provided the best curve fit for all of the data. The third factor that may affect agreement between the test data and the prediction curves is the size of the hole radius in relation to the size of the parameter d. For example, the data on Fig. 8b for the 2.5-cm-wide specimens correlates well for holes greater than about 1 cm in diameter, but, specimens with smaller holes have a lower strength than predicted. Holes with an a/w ratio of 0.1 have a hole radius about the same size as the value of d. This is also true for the 5.1-cm-wide specimens with an a/w ratio of 0.05. An examination of the stress distribution in Fig. 2 indicates that the stress concentration for small holes is significantly reduced one radius from the hole edge. Therefore, the point-stress failure

prediction criterion may not be applicable when the radius of the hole in the specimens is about the same size as the value of d.

The effect of matrix resin on the failure strain of panels with drilled holes is shown in Fig. 9. These specimens were fabricated from material B and are identified as specimen B1 in Table 3. Results in Fig. 9 compare very favorably with the prediction curve for the material A panels from Fig. 8. This indicates there is little effect of resin on the failure of panels with holes, which is somewhat surprising because there was considerable difference in the failure strain of these material systems due impact damage.[3] The current results from the panels with holes probably indicate similar failure mechanisms associated with the hole failures which may be different from those associated with impact damage. Failures observed in panels with holes will be discussed in a subsequent section.

Effect of Ply Orientation on Quasi-Isotropic Laminates

Limited tests were conducted on quasi-isotropic laminates of material A with fiber orientations of $(\pm 60/0/\mp 60/0)_{4s}$ and $(\pm 30/90/\mp 30/90)_{4s}$. The results from these tests are shown in Fig. 10. The format of Fig. 10 is the same as that of Fig. 8 and the failure prediction curve from that figure for the $(\pm 45/0/90/\mp 45/0/90)_{3s}$ laminate is also shown. The test results for the $(\pm 60/0/\mp 60/0)_{4s}$ laminate compare favorably with the predicted failure curve, while the results for the $(\pm 30/90/\mp 30/90)_{4s}$ laminate indicate these specimens had failure loads below those of the order two quasi-isotropic ply orientations evaluated. The $(\pm 30/90/\mp 30/90)_{4s}$ laminate is not loaded in the direction of any filament orientation and consequently the ultimate strength of the laminate may be controlled by a mechanism other than filament strength. However, the trends of the $(\pm 30/90/\mp 30/90)_{4s}$ are similar to those of the other test laminates.

Orthotropic Laminates with Holes

The applied strain at failure for the orthotropic specimens is shown in Fig. 11 as a function of hole size for several panel widths (specimens A6-A9 in Table 3 and data from Refs. 13 and 17). The format of Fig. 11 is the same as that of Fig. 8. The predicted failure curves determined using the stress distributions of Fig. 2b are shown on Fig. 11a for three values of d. The value of $d = 0.05$ cm appears to be the best fit failure prediction curve for the selected value of ultimate material strain of 0.014. The value of ultimate strain is known to vary for different laminates, however, an accurate value of ultimate strain was not determined in this experimental study. The test data for all panel widths agree with the prediction curves with the exception of one point on Fig. 11b which will be discussed subsequently. The agreement between the test data and predicted failure results in both Figs. 8 and 11 for laminates of different orthotropic properties demonstrates the potential for the point-stress failure criteria as a useful prediction technique and its value in understanding and interpreting test results. However, the combination of d and ultimate material strain used to fit the test results of Fig. 11 is not unique and a different combination of ultimate strain and d also can be shown to fit these test results. The implication of using other parameter combinations will be discussed in a subsequent section.

The failure strain for test panel A9 with an a/w ratio of 0.2 shown on Fig. 11b is below the notch sensitive curve which suggests that the failure is controlled by a mechanism other than material strength. The 7.6-cm-diameter hole in that panel is a relatively large diameter unreinforced hole for a 0.67-cm-thick panel. The specimen was supported at the one-third points to suppress a panel buckling mode of one-half wave length across the specimen width. However, other modes of shorter wavelength may have occurred during the test, including local buckling near the hole perimeter due to the high stresses in the vicinity of the hole. Test results presented in Ref. 19 indicated that several 48-ply panels evaluated in that study failed at buckling and the applied strain at failure for the Ref. 19 panels, although not shown, are below the predicted notch sensitive curve of Fig. 11. The additional bending strain due to buckling is probably adequate to cause failure to occur in test panel A9. Tests to investigate local bending strains near a hole in compression panels loaded into the post-buckling range are reported in Ref. 21.

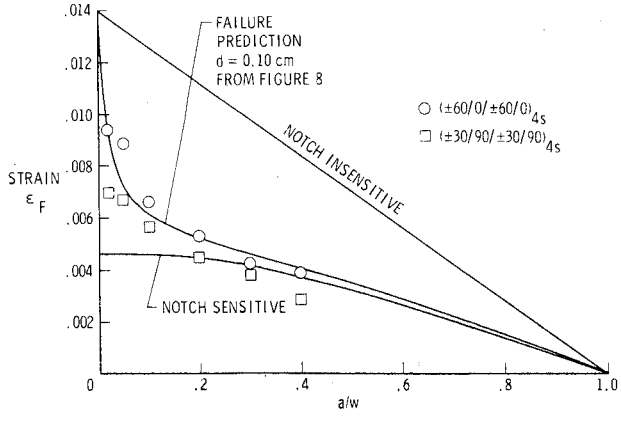

Fig. 10 Failure strain of quasi-isotropic laminates with different ply orientations as a function of hole size (material A).

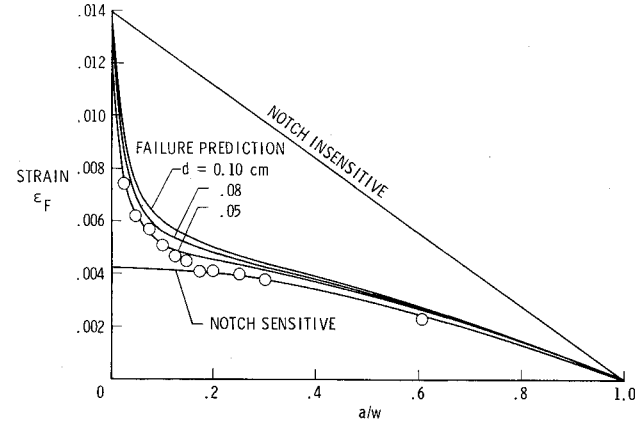

a) 12.7-cm-wide test panels, Ref. 17.

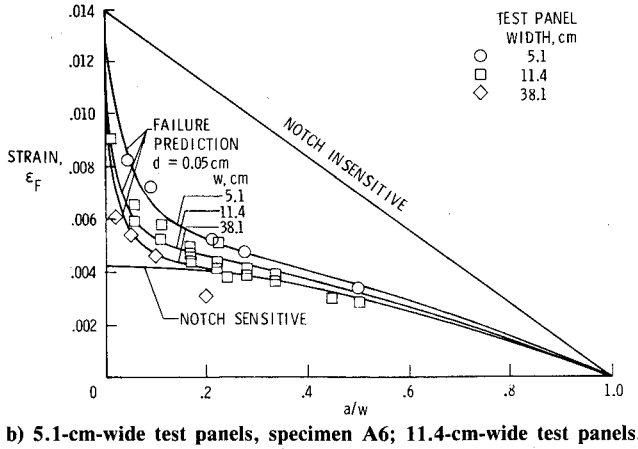

b) 5.1-cm-wide test panels, specimen A6; 11.4-cm-wide test panels, specimen A7 and results from Ref. 13; and 38.1-cm-wide test panels, specimens A8 and A9.

Fig. 11 Failure strain of an orthotropic laminate as a function of hole size (material A).

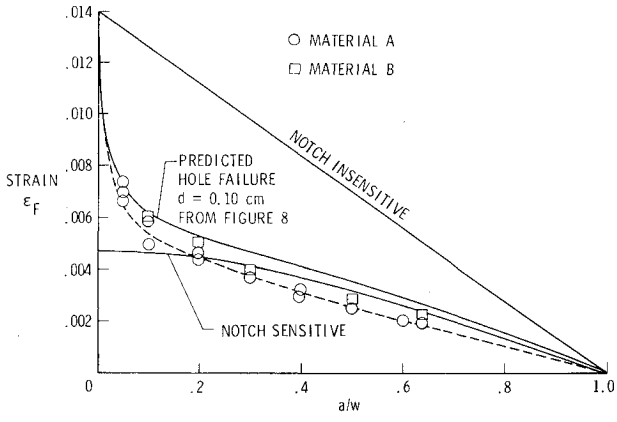

Fig. 12 Failure strain of 12.7-cm-wide quasi-isotropic plates with machined cracks as a function of crack width.

Quasi-isotropic Laminates with Cracks

The applied strain at failure for panels with machined cracks is shown in Fig. 12. These panels are quasi-isotropic laminates fabricated from materials A and B and are identified as specimens A10 and B2 in Table 3. The figure format is the same as that of previous figures. A dashed curve has been faired through the data points to illustrate the trend and aid in comparing test results with the predicted hole failure curve from Fig. 8. There is no appreciable difference in the failure strain of panels fabricated from these two material systems. The test results in Fig. 12 for these finite width plates substantiate the previous analysis discussion which was based on infinite width plates. That analysis postulated that for small holes and cracks the strain at failure would be about the same, while large cracks would have a lower applied strain at failure than a hole of a similar diameter. Accurate stress distributions for cracks in infinite width plates will be required to predict failure and determine if the d parameter for cracks is the same as that for holes.

Evaluation of Punched Holes

The effect of hole quality on the failure strain of a quasi-isotropic laminate (specimens A13 and B3 in Table 3) is shown in Fig. 13. The holes were punched in the test panels using a conventional hydraulic press and there was obvious damage in the panel material around the hole from the punching operation. The data are shown as a function of the nominal punch diameter and the diameter of a circle adequate to encompass all the damage inflicted as a result of the punching operation, including delamination, as determined by ultrasonic inspection. Also shown on Fig. 13 is the failure prediction curve for holes in 12.7-cm-wide plates and the curve faired through the data from the specimens with machined cracks (Fig. 12).

The curve from the panels with machined cracks fits the test data on Fig. 13a for material A based on the diameter of the damaged area as determined by ultrasonic inspection, and the data on Fig. 13b for material B based on the nominal punch diameter. The data for material A based on the nominal punch diameter falls below any of the curves on the figure, including the notch sensitive curve. Material A contains a brittle resin system and there is more delamination damage introduced by the punching operation than material B which contains a ductile resin system (note neat resin elongation to failure, Table 1). Although these test results are preliminary, they suggest that predicted failure of graphite-epoxy composite panels with fiber damage of an irregular nature, such as impact or an accidental punch through, probably should be evaluated on the more conservative basis of a crack rather than a hole.

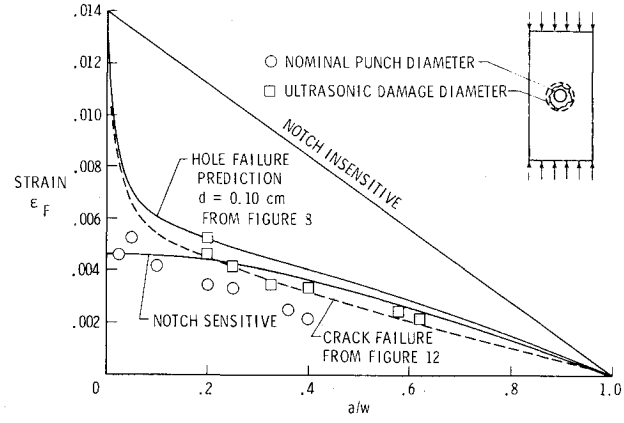

a) Plates fabricated from material A.

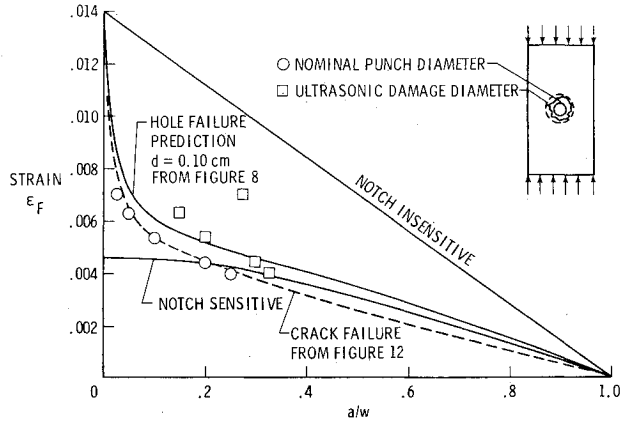

b) Plates fabricated from material B.

Fig. 13 Effect of hole quality on the failure strain of a quasi-isotropic laminate.

Sequence of Failure Events

In observing the failure of compression loaded panels with holes it was frequently noted that in approaching the failure load local protuberances would develop near the edge of the hole. Several test panels with holes were loaded in compression to a value estimated to be near failure. These specimens subsequently were cross sectioned, plies were removed with abrasive paper, and the surfaces were examined microscopically.

Failures typical of those observed in the test panels are shown in Fig. 14. Panels loaded to approximately 85% of the predicted failure load exhibited only interfiber matrix failure in the 0° plies (see Fig. 14a). The fibers cut during the drilling operation are separated from the uncut fibers for some small distance adjacent to the holes. Panels with only these failures had no evidence of broken fibers. The interfiber matrix failure is probably a shear failure of the matrix due to the high-stress gradient in the vicinity of the hole. Specimens loaded to a higher percentage of the predicted failure load had regions of shear crippling in the 0° plies near where the interfiber matrix failure terminated (see Figs. 14a and 14b). Shear crippling such as this was observed frequently in several 0° plies through the thickness. The shear crippling causes a distortion or wedging action of the fractured fibers to develop between the 0° plies and the adjacent angle plies of the laminate. This is probably responsible for the development of local protuberances near the hole edge noted previously. An estimate was made of the distance from the edge of the hole to the point where the shear crippling failure was initiated. This distance was about the same as the values of d used in the point-stress failure prediction technique for

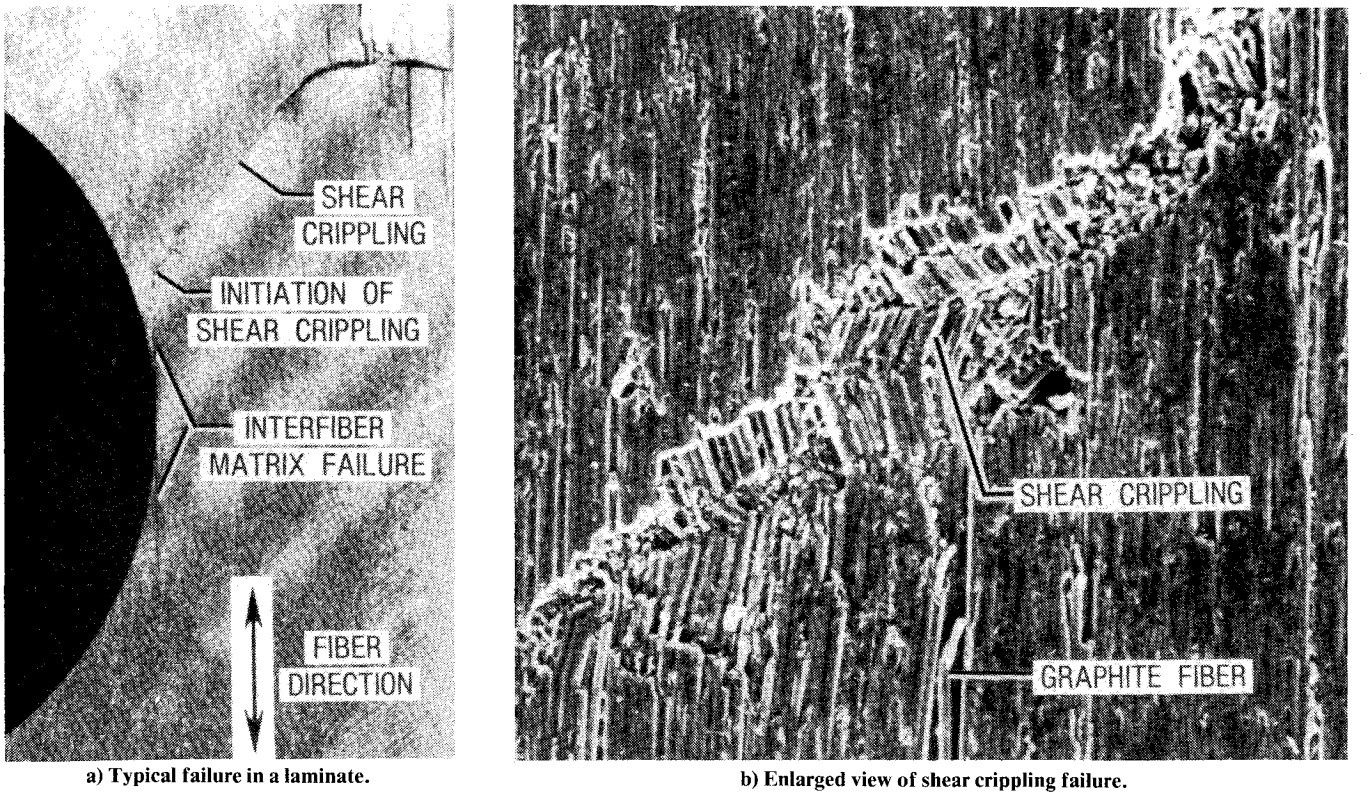

a) Typical failure in a laminate.

b) Enlarged view of shear crippling failure.

Fig. 14 Intralaminar failures in 0° plies near hole edge.

the test laminates. No attempt, however, was made to determine this distance accurately and correlate the measurement with the value of d used to curve fit the data with the failure prediction technique.

Discussion

The point-stress failure criterion is a prediction technique whose correlation depends upon the accurate evaluation of two independent parameters, the ultimate strength of the material and the value chosen for d. However, if one of these independent parameters can be fixed for certain cases, the technique can be applied after evaluation of only one parameter which might be determined by a few carefully chosen tests. A theory can be advanced for holding the ultimate strain of the material constant making d the independent parameter, and a theory likewise can be advanced for holding d constant making the material strength (or failure strain) the independent parameter. Issues associated with each of these theories are discussed in the following paragraphs.

It was proposed in Ref. 5 that d, once determined, should be held constant and considered a material property. The value of d then would be independent of laminate geometry and local stress distribution. The rationale for this premise was that d is analogous to the stress intensity factor used in fracture mechanics which is considered to be a material property; and that material strength, which varies with laminate orientation, was controlled by nonlinear matrix behavior and was affected by stress interaction within the laminate. The experimental data for the laminates evaluated in this investigation (Figs. 8 and 11) were compared with prediction curves based on a value of $d=0.10$ cm for the quasi-isotropic laminate and a value of $d=0.05$ cm for the orthotropic laminate. Prediction curves were also obtained using a value of $d=0.10$ cm for the orthotropic data and an ultimate strain of 0.012. The curves based on $d=0.10$, although not shown, provided a data fit similar to that shown in Fig. 11.

The data presented in this paper was analyzed on the basis of holding the ultimate strain of the material constant making d the independent variable. Most of the laminates evaluated were filament controlled, i.e., they have several plies with filaments in the direction of the applied load. This failure premise is that laminate failure occurs when the applied strain reaches the failure strain of these filaments. The failure observed in the microscopic analysis tends to support this theory because shear crippling of the 0° filaments was apparently the mechanism associated with laminate failure.

Narrow test specimens with holes are frequently used in ancillary test programs to develop design data. These specimens are typically 2-3 cm wide and are selected to keep both material costs and test frame load requirements low. The data presented in Fig. 8 suggest that narrow specimens do not give an accurate indication of material notch sensitivity nor will they yield parameters that accurately predict failure if small holes are used to determine the parameter d. Therefore, several specimen widths with large holes in comparison to d should be included in any test program to develop general prediction trends for use in design-type applications.

The results presented herein indicate that the point-stress failure criterion can be an effective tool in predicting and understanding the failure of graphite-epoxy composite laminates with holes, and provides insight in predicting failure of panels with other flaw types. Although the use of this technique for finite width panels requires a complex analysis to calculate the stress distributions and stress concentrations for different hole diameter-to-specimen width ratios, the application is simple and can be presented in a design chart format. The results presented herein represent a first step in developing a general failure prediction technique for compression loaded structures with damage.

Concluding Remarks

An experimental study was conducted to evaluate the effect of laminate orthotropic properties and panel width on the compression strength of graphite-epoxy laminates with holes.

Tests were conducted on 48-ply specimens of several different ply orientations, all of which were fabricated from unidirectional tape materials. The test results were evaluated on the basis of hole size and specimen width and were used to determine parameters necessary to predict trends using the point-stress failure criterion. The point-stress failure criterion is based on the assumption that failure occurs when the stress at some small distance from the hole edge reaches the ultimate strength of the material. It is a heuristic technique that accounts for local effects in the region of high-stress concentration adjacent to the hole, and was used in the current investigation as a convenient prediction technique.

The point-stress failure criterion was applied to both quasi-isotropic and orthotropic panels and the results indicate that the point-stress criterion can be a very useful technique in predicting and interpreting test results. Both plate width and hole diameter have a significant (but predictable) effect on compression strength. The test results were shown to be bounded below by material failures that are initiated by stress concentration only, and above by material failures that are controlled by the reduction in the area of the specimen cross section. Increasing specimen width results in panels being more sensitive to the effects of stress concentrations. This may affect the interpretation of test results, particularly if narrow panels (2-3 cm wide) are used to develop design data which is frequently the case in ancilliary test programs. Also narrow panels with small holes (the hole radius is about the same size as the distance to the point where the stress is assumed to reach a critical value) should not be used exclusively to define the correlation parameter for the point-stress failure prediction criterion.

Results of tests on quasi-isotropic laminates with different ply orientations indicate that those laminates that have plies in the direction of the applied load exhibited similar failure trends. However, those that did not have plies in the direction of the applied load failed at a lower applied strain. The laminate that failed at the lower applied strain is probably controlled by a mechanism other than filament strength.

Quasi-isotropic panels with machined cracks were tested and the results compared to the panels with holes. This comparison shows that panels with small cracks fail at about the same applied strain as those with holes, however, panels with large cracks fail at a lower value of applied strain than a panel with a hole of the same size.

The sequence of falure events that occurs in the vicinity of a hole for panels loaded to a value estimated to be near failure was identified. This was determined by microscopically examining plies in several panels loaded to different percentages of the estimated failure load. The first failure was observed in panels loaded to about 85% of the estimated ultimate load and is an interfiber matrix failure in the plies oriented in the direction of the applied load. Specimens loaded to a higher percentage of ultimate load had shear crippling failures in plies of the same orientation and the shear crippling failures were initiated near where the interfiber matrix failure terminated. The shear crippling resulted in specimen failure and was probably the dominant mechanism associated with failure in most of the test panels.

References

[1] Rhodes, M. D., Williams, J. G., and Starnes, J. H., Jr., "Low-Velocity Impact in Graphite-Fiber Reinforced Epoxy Laminates," *Reinforcing the Future*; Proceedings of the 34th Annual Conference, New Orleans, La., Jan. 30-Feb. 2, 1979. Society of the Plastics Industry Inc., New York, N.Y., 1979, p. 20-D1 to 20-D10.

[2] Byers, B. A., "Behavior of Damaged Graphite/Epoxy Laminates Under Compression Loading," NASA CR-159293, 1980.

[3] Rhodes, M. D. and Williams, J. G., "Concepts for Improving the Damage Tolerance of Composite Compression Panels," NASA TM 85748, Feb. 1984.

[4] Waddoups, M. E., Eisenmann, J. R., and Kaminski, B. E., "Macroscopic Fracture Mechanics of Advanced Composite Materials," *Journal of Composite Materials,* Vol. 5, Oct. 1971, pp. 446-454.

[5] Whitney, J. M. and Nuismer, R. J., "Stress Fracture Criteria for Laminated Composites Containing Stress Concentrations," *Journal of Composite Materials,* Vol. 8, July 1974, pp. 253-265.

[6] Nuismer, R. J. and Labor, J. D., "Applications of the Average Stress Failure Criterion: Part I—Tension," *Journal of Composite Materials,* Vol. 12, July 1978, pp. 238-249.

[7] Garbo, S. P. and Ogonowski, J. M., "Strength Predictions of Composite Laminates with Unloaded Fastener Holes," AIAA Paper 79-0800, 1979.

[8] Nuismer, R. J. and Labor, J. D., "Applications of the Average Stress Failure Criterion: Part II—Compression," *Journal of Composite Materials,* Vol. 13, Jan. 1979, pp. 49-60.

[9] Garbo, S. P., "Compression Strength of Laminates with Unloaded Fastener Holes," AIAA Paper 80-0709, 1980.

[10] Mikulas, M., Jr., "Failure Prediction Techniques for Compression Loaded Composite Laminates with Holes," Selected NASA Research in Composite Materials and Structures, NASA CP 2142, Seattle, Wash., Aug. 1980.

[11] Palmer, R. J., "Investigation of the Effect of Resin Material on Impact Damage to Graphite-Epoxy Composites," NASA CR 165677, March 1981.

[12] Williams, J. G. and Rhodes, M. D., "The Effect of Resin on the Impact Damage Tolerance of Graphite-Epoxy Laminates," NASA TM 83213, Oct. 1981.

[13] Starnes, J. H., Jr., Rhodes, M. D., and Williams, J. G., "Effect of Impact Damage and Holes on the Compressive Strength of a Graphite/Epoxy Laminate," Nondestructive Evaluation and Flaw Criticality for Composite Materials, ASTM STP 696, edited by R. B. Pipes, American Society for Testing and Materials, Philadelphia, Pa., 1979, pp. 145-171.

[14] Tang, S., "Interlaminar Stresses Around Circular Cutout of Composite Plates Under Tension," AIAA Paper 77-409, 1977.

[15] Timoshenko, S. and Goodier, J. N., *Theory of Elasticity,* 2nd Ed., McGraw-Hill Book Co., New York, 1951.

[16] Hong, C. S. and Crews, J. H., Jr., "Stress-Concentration Factors for Finite Orthotropic Laminates with a Circular Hole and Uniaxial Loading," NASA 1469, May 1979.

[17] Greszczuk, L. B., "Stress Concentrations and Failure Criteria for Orthotropic and Anisotropic Plates with Circular Openings," Composite Materials: Testing and Design (Second Conference), ASTM STP 497, American Society for Testing and Materials, Philadelphia, Pa., 1972, pp. 363-381.

[18] Sneddon, N., *Fourier Transforms,* McGraw-Hill Book Co., New York, 1951.

[19] Knauss, J. F., Starnes, J. H., Jr., and Henneke, E. G., II, "The Compressive Failure of Graphite/Epoxy Plates with Circular Holes," NASA CR-157115, Feb. 1978.

[20] Vaughn, R. L., "Flight Service Evaluation of an Advanced Composite Empennage Component on Commercial Transport Aircraft," NASA CR-159286, April 1976.

[21] Starnes, J. H., Jr. and Rouse, M., "Postbuckling and Failure Characteristics of Selected Flat Rectangular Graphite-Epoxy Plates Loaded in Compression," AIAA Paper 81-0543, 1981.